Design of an L-Band Microwave Radiometer with Active Mitigation of Interference

Steven W. Ellingson, G.A. Hampson, and J.T. Johnson
The Ohio State University ElectroScience Laboratory
1320 Kinnear Rd., Columbus, OH 43212
{ellingson.1, hampson.8, johnson.1374}@osu.edu

Abstract— **For increased sensitivity in L-band radiometry, bandwidths on the order of 100 MHz are desirable. This will likely require active countermeasures to mitigate RFI. In this paper, we describe a new radiometer which coherently samples 100 MHz of spectrum and applies real-time RFI mitigation techniques using FPGAs. A field test of an interim version of this design in a radio astronomy observation corrupted by radar pulses is described. Measurements of the radio frequency environment at L-band from an airborne system are also discussed.**

I. Introduction

Radio frequency interference (RFI) impairs the operation of L-band radiometers, particularly outside the protected 26 MHz frequency band around 1413 MHz. However, bandwidths on the order of 100 MHz are desirable at L-Band to improve sensitivity in applications such as soil moisture and ocean salinity sensing. Because much of the RFI in this band is from radars with pulse lengths on the order of microseconds, traditional radiometers (i.e., those which directly measure total power integrated over time scales of milliseconds or greater) are poorly-suited to this task. This motivates the design and development of radiometers capable of coherent sampling and adaptive, real-time mitigation of interference.

Since December 2001, we have been working to develop such a radiometer. Our design, described in Section II, is capable of coherently sampling 100 MHz at L-band, with real-time RFI mitigation implemented using field-programmable gate array (FPGA) devices. In Section III, we describe a test of an interim implementation of our design in an L-band radio astronomy application.

To provide additional information on the radio frequency interference environment at L-band, we have also been performing surveys with an airborne instrument. Section IV provides further information on these studies, while Section V describes the instrument used in detail. Sections VI and VII describe survey results, and a discussion of project implications for L-band radiometry is provided in Section VIII.

II. Radiometer Design

A block diagram of our radiometer is shown in Figure 1, and a picture of the digital section is shown in Figure 2. The analog front end downconverts an 80 MHz swath of spectrum from L-band to 150 MHz, and samples this signal at 200 MSPS using 10 bits. Because the

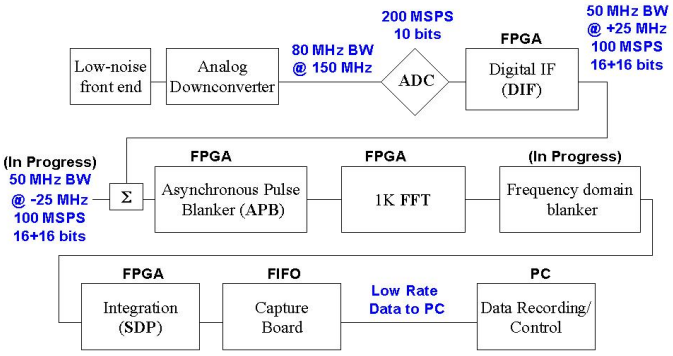

Fig. 1. Block diagram of radiometer.

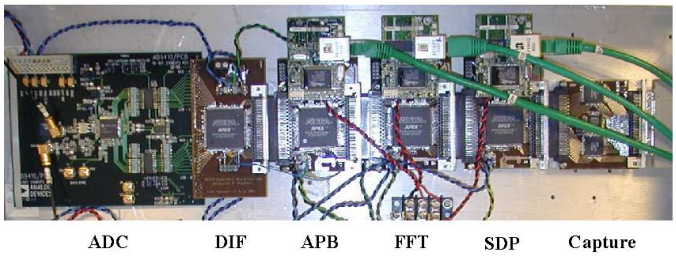

Fig. 2. The interim digital design as used in the November 2002 experiment described in Section III. Since then, the ADC has since been replaced with a smaller custom board. Also, a number of the Altera APEX-series FPGAs shown here have been replaced with Altera Stratix FPGAs, including the DIF (which now supports two 50-MHz channels) and the FFT; see text.

analog IF is in the second Nyquist zone of the A/D, the digital passband is centered at 50 MHz and is spectrally reversed. The "Digital IF" (DIF) FPGA module downconverts this to 0 Hz (so now the samples are complex-valued), filters to 50 MHz bandwidth, decimates by 2, and then upconverts to a center frequency of +25 MHz (still complex). The data emerges from the DIF module in 16-bit "I" + 16-bit "Q" format at 100 MSPS. The same process is applied to a separate, independently-tunable 50-MHz swath at L-Band, with the difference that the digital output is centered at −25 MHz. The two 50 MHz bands are simply added together to form a single 100 MHz bandwidth signal.

Following the DIF output is a cascade of FPGA modules which can be programmed to perform a variety of functions. Our favored strategy currently is as shown in

Figure 1: mitigation of radar pulses using asynchronous pulse blanking (APB, described below), channelization into 100-kHz bins using a 1K FFT, frequency domain blanking, and integration to generate power spectra.

The APB is designed to detect and blank radar pulses, which typically are the dominant source of external L-Band RFI below 1400 MHz. Radar pulses range from 2–400 μs in length and occur 1–75 ms apart [1]. To detect these pulses, the APB maintains a running estimate of the mean and variance of the sample magnitudes. Whenever a sample magnitude greater than a threshold number of standard deviations from the mean is detected, the APB blanks (sets to zero) a block of samples beginning from predetermined period before the triggering sample, through and hopefully including any multipath components associated with the detected pulse. (A future version of this algorithm will probably implement some form of matched filtering to improve detection performance.) APB operating parameters are adjustable and can be set by the user; see Section III for an example.

Following the APB is a length-1K complex FFT. The original implementation had an effective duty cycle of 19% (i.e., 19% of the data was FFTed, and the rest is lost). In January 2003 this module was upgraded and now achieves $\sim$ 98% duty cycle. A triangular window is applied before the FFT. Planned but not yet implemented is a frequency-domain blanking module, which is similar in concept to the APB, except applied independently to each frequency bin. The purpose of this module will be to exploit the processing gain achieved through channelization to detect and excise weak, relatively narrowband RFI. The FFT output is processed through a "spectral domain processor" (SDP) module which computes magnitude-squared for each frequency bin and computes a linear power average over many FFT outputs. These results are passed at a relatively low rate to a PC via a capture board. Total power can be computed by summation of frequency bins within the digital hardware, or the same process can be implemented within the PC for increased flexibility in monitoring RFI, selecting subbands, and so on.

Beyond considerations of RFI mitigation, this architecture has additional advantages over traditional radiometers. Because the noise level is positioned in the low-order bits of the A/D (primarily to allow headroom for strong RFI), only about 50–60 dB gain is required from the front end. Relative to radiometers requiring 100 dB or more of front end gain, this dramatically improves stability in the presence of temperature variations. Also, the final 50-MHz-wide IF filter is digital, and significantly narrower than the final analog filter, which is 80 MHz wide. Figure 3 demonstrates results from an initial stability test of this design through observation of an ambient temperature load (not thermally stabilized.)

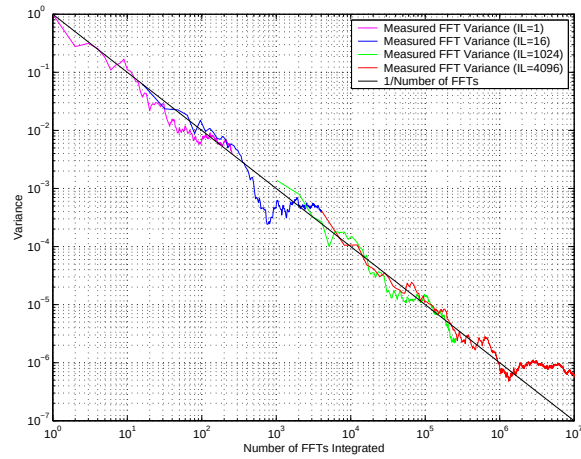

Fig. 3. Noise variance vs. time for the radiometer when terminated by a matched load at the input. This observation represents 100 s of integration over 14 min elapsed time. No calibration, temperature control, or Dicke switching of any kind was employed.

III. On-The-Air Testing at Arecibo

In November 2002, we had an opportunity to test the RFI mitigation capabilities of the radiometer by "piggybacking" on a radio astronomical observation at the Arecibo (Puerto Rico) Observatory. L-band radio astronomy, like remote sensing, is plagued by RFI; in particular, interference from radars in the 1215–1400 MHz band. Our radiometer was connected to the telescope through a spare IF output at $\sim$ 250 MHz, which we upconverted back to L-band for input into our system. At the time, we had only one of the two 50 MHz subbands constructed. The SDP was configured to compute linear power averages over 4096 length-1K FFT outputs, for an effective integration time of $\sim$ 221 ms. After 254 of these spectra were collected in a FIFO, the data were transferred to the PC and the experiment terminated.

The APB was configured as follows:

- Trigger on sample magnitudes greater than $\sim 10\sigma$ above the mean.
- Start blanking 100 samples (1 μs) in advance of the triggering sample.
- Blanking period is 100 μs long.
- Wait at least 44 μs between triggers (attempting to prevent multiple triggers on the same pulse).

These parameters were selected based on some known properties of a strong radar visible at Arecibo [2], and no attempt was made to optimize these parameters based on the observed data.

Measurements were taken at three center frequencies: 1255 MHz, 1300 MHz, and 1350 MHz; in each case, we performed the measurement once with the APB disabled, and then again with the APB on. The 1350 MHz results are shown in Figure 4. These spectra represent $\sim$10.7 s of

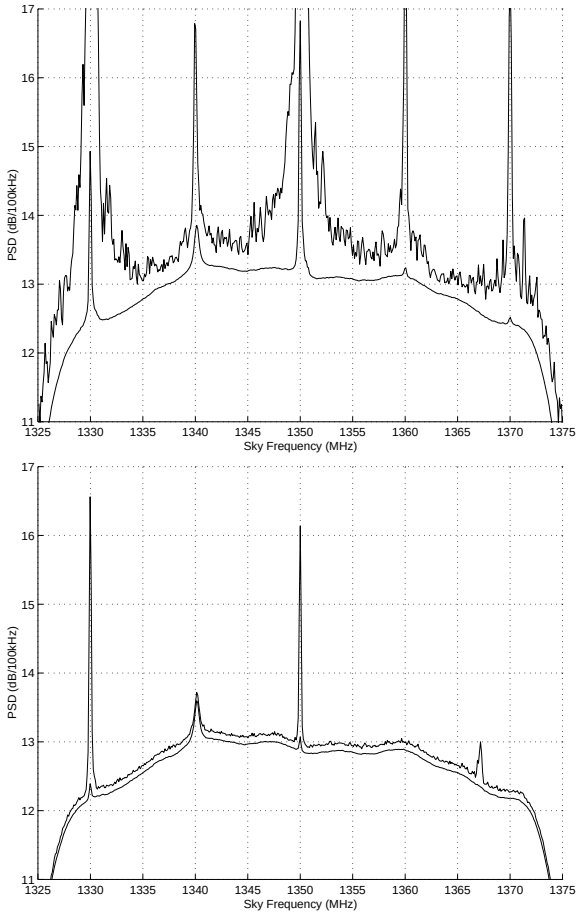

Fig. 4. Mean and max-hold spectra. *Top Panel:* APB off; *Bottom panel:* APB on.

integration in ∼42 ms segments evenly distributed over ∼56 s in real time. Also shown in Figure 4 is the "max hold" of the 42-ms spectra. The max hold spectra are computed by taking for each frequency bin the maximum value observed in that bin over the course of the experiment. Max hold spectra are useful for revealing bursty signals (especially radars) which tend to be suppressed in deep integrations due to their low duty cycle.

With the APB off, we observe strong RFI at 1330 and 1350 MHz (these are in fact transmitted from the same radar), plus a few other frequencies. The front end of the telescope's receiver is driven into compression when the 1330/1350 MHz radar is pointed near Arecibo, which occurs every ∼ 11 s and accounts for the ragged max hold spectrum. When the APB is turned on, we see a dramatic improvement in the sense that large portions of the spectrum are salvaged. In this case, we found that ∼ 5% of the data was blanked by the APB.

Note that 1330/1350 MHz radar is not completely suppressed by the APB. The reason for this is that the version of the APB algorithm used here assumes that only

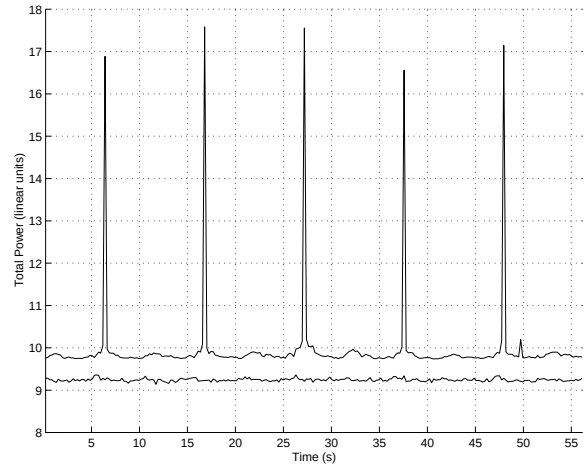

Fig. 5. Time domain total power. *Top:* APB off; *Bottom:* APB on.

one radar is present at a time. As a result, a relatively weak radar pulse can distract the APB from a stronger radar pulse occurring later within the specified blanking period. This shortcoming has subsequently been corrected.

Figure 5 shows total power in 50 MHz bandwidth as a function of time. The ∼11 s rotation period of the 1330/1350 MHz radar is clearly evident in the APB-off data. When the APB is turned on, the radar appears to be completely removed. The performance appears to be better in this case because the residual shown in the lower panel of Figure 4 is limited to a very small faction of the processed time-frequency space, and thus becomes insignificant compared to the total noise power available in the band. We conclude that even simple blanking schemes as used here show great promise for use in total-power radiometry.

IV. L-band RFI Survey

Although initial results from the Arecibo measurement are promising, further improvements should be possible through appropriate choices of the parameters of the RFI mitigation algorithms. Choosing these parameters as well as designing new mitigation strategies requires detailed information on properties of the RFI environment. Information on the RFI environment over a range of geographical locations is also of interest for developing and testing mitigation strategies for a future satellite borne sensor.

To address this issue, surveys of RFI in the frequency range 1200-1800 MHz have been performed from an airborne platform. The data were collected using a portable instrument known as the L-Band Interference Surveyor/Analyzer (LISA), which was developed at the Ohio State University ElectroScience Laboratory in 2002.

LISA includes two complementary subsystems: an off-the-shelf computer-controlled spectrum analyzer and a custom wideband high-dynamic-range coherent-sampling receiver. The former is useful for understanding the distribution of RFI over large frequency spans and long time periods, whereas the latter provides waveform capture capability with high temporal resolution. The data discussed was taken in an initial test flight above the mid-Atlantic coast of the US. Although the digital receiver backend of the radiometer discussed in Section II could also provide waveform capture capability, the LISA wideband receiver was based on an earlier radio-astronomy system due to time and scheduling issues.

A technical report including additional details about LISA and the measurements described below is available from the authors.

V. Instrumentation and Experiment Conditions

LISA is designed to observe and record RFI in the 1200–1800 MHz band. The antenna unit consists of a nadir-facing cavity-backed planar spiral antenna with an integrated custom RF front end including filtering and calibration circuitry. The antenna has a very broad pattern (approximately "$\cos\theta$") and is reasonably well-matched over the span of the observations reported here. The antenna unit is connected to an equipment rack mounted in the aircraft cabin by a long and fairly lossy coaxial cable. Although the cable loss degrades the sensitivity of the instrument, the resulting gain profile was an important factor in preserving the linearity of the system while observing strong RFI. Since one of our goals was to coherently sample RFI waveforms, this consideration was paramount, but comes at the expense of the system's ability to detect weak RFI.

Inside the equipment rack, a portion of the 1200-1800 MHz signal is coupled to a PC-controlled spectrum analyzer. The spectrum analyzer is used to perform either a "max hold" or "linear average" measurement. The remainder of the signal is delivered to the custom-designed coherent sampling subsystem. This subsystem uses a direct-conversion receiver to tune (under PC control) anywhere between 1200 MHz and 1700 MHz. "I" and "Q" signals at baseband are low-pass filtered with $\sim$ 7 MHz cutoff and sampled at 20 MSPS, yielding a digitized bandwidth of $\sim$ 14 MHz. The output samples are queued in a 16K-sample-long first-in-first-out (FIFO) buffer, providing 819.2 μs of contiguous signal capture. The FIFO contents are acquired by means of the PC parallel port. During the test flight, the coherent sampling system was successively tuned through center frequencies of $1250, 1264, \cdots, 1698$ MHz, with 5 acquisitions in a period of approximately 5 seconds before tuning to the next center frequency.

For the experiment described here, LISA was installed in NASA's P-3 research aircraft, which is based at the Wallops Flight Facility (WFF) located at Wallops Island, VA. The LISA antenna unit was mounted in the tail radome. The loss due to transmission through the radome is unknown (hence, not taken into account in the calibrated measurements presented here) and may be another factor degrading sensitivity.

The data presented below were collected during a single flight on January 2, 2003 in the vicinity of the WFF.[1] The flight consisted of two phases. In Phase I, the aircraft flew a pattern consisting of mostly straight lines at approximately 20,000 ft over open ocean, a short distance east of the Maryland / Delaware coast. In Phase II, the aircraft flew along an east-west track in the vicinity of Exmore, VA (approx. 37.5° N lat, 75.7° W long) at 2000 ft, returning along the same track.

VI. Spectrum Analyzer Results

Phase I Results (20,000 ft over Open Ocean): Summary results for 1320–1420 MHz using the spectrum analyzer are shown in Figure 6. Immediately apparent is the profusion of RFI below 1370 MHz. Some of the RFI is quite strong, generating bursts of power well above -40 dBm at the antenna terminals in some cases. It is also clear that most or all of the detected interference is bursty in nature. This is can be deduced by noting the relative lack of detections in the linear average trace relative to the max hold trace. The signals that are apparent in the linear average trace are most likely strong, pulsed signals that were reduced, but not eliminated, by averaging. Considering that the much of the spectrum below 1400 MHz is allocated for ground-based radar, the observed data suggest that most of the observed signals are in fact radars.

Important to note is that this data represents only 18 passes through the spectrum over a 74 min time period. Since the transmit duty cycle of most radars is on the order of 0.1%, it is likely that there are a great many additional pulses that are missed due to the low observing duty cycle.

The apparent RFI visible between 1395–1407 MHz in Figure 6 is to date unidentified. Certainly, no external RFI is expected in the 1400–1427 MHz band, but neither does the observed RFI appear to be internal.

Although space limitations preclude their presentation here, spectra covering the entire 1200–1800 MHz band with various resolution bandwidths were obtained and similarly analyzed. No significant external RFI was detected above 1420 MHz in this data.

[1] LISA was also operated during the January 2003 portion of the Wakasa Bay (Japan) AMSR-E campaign, including portions of the transit flight from WFF. At present, analysis of data from these flights is not yet complete.

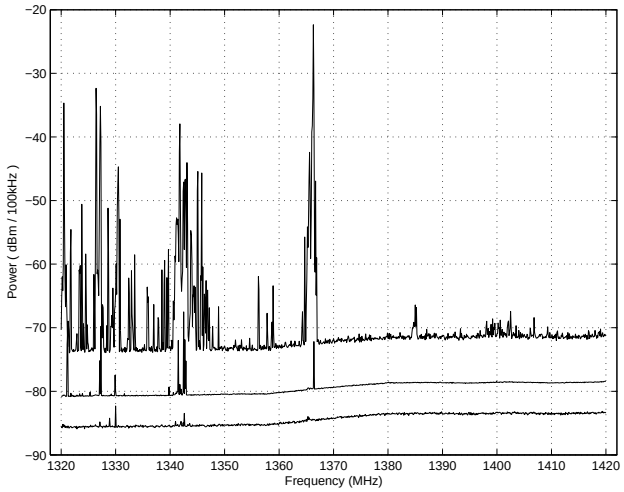

Fig. 6. Summary spectrum analyzer results for 20,000 ft. *Top:* Max hold, antenna; *Middle:* Linear average, antenna; *Bottom:* Linear average, calibration load minus 5 dB for clarity. Power in 100 kHz referenced to antenna terminals. The bottom trace represents 10% of the integration time of represented in the antenna traces.

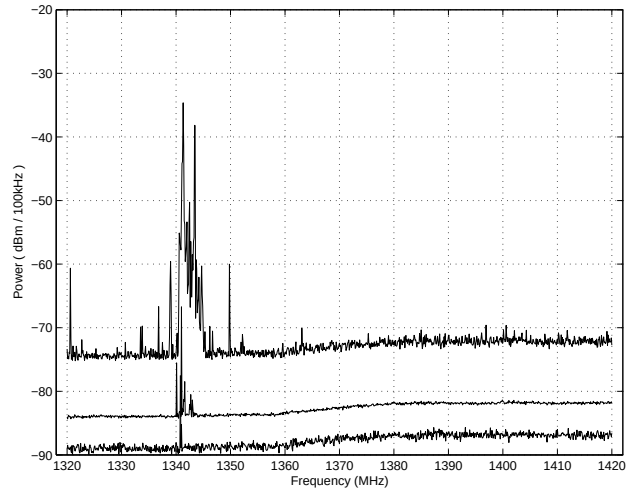

Fig. 7. Summary spectrum analyzer results for 2,000 ft. *Top:* Max hold, antenna; *Middle:* Linear average, antenna; *Bottom:* Linear average, calibration load minus 5 dB for clarity. Power in 100 kHz referenced to antenna terminals. Note that the terminator trace represents 10% of the integration time of represented in the antenna traces. The reason for the slight change in the levels of the lower two traces relative to Figure 6 is not known.

Phase II (2,000 ft over Exmore, VA): Summary results for spectrum analyzer observations are shown in Figure 7. Relative to the Phase I data, there are fewer signals detected, and those that remain seem weaker. This may be because much more of the surface of the Earth is within line of sight (LOS) from 20,000 ft relative to 2,000 ft, resulting in a greater number of detectable transmitters within LOS as well.

Although not apparent in Figure 7, scans using other spectrum analyzer configurations (wider resolution bandwidth) revealed RFI in the 1395–1407 MHz range similar to that seen in Figure 6. As in the Phase I data, no external RFI was detected above 1420 MHz.

VII. Coherent Capture Results

Coherent sampling was used at 20,000 ft (during Phase I) only. To identify RFI in the captured data, each 16K sample block was visually examined in the time domain as a single trace representing all 14 MHz of captured bandwidth. Eight interference-bearing blocks were unambiguously identified out of 615 total acquisitions. In all 8 cases, summarized in Figure 8, the interference consisted of a single pulse of either 2 μs or $\sim$ 60 μs duration, plus resolved multipath in two cases. It appears that 6 separate radars are involved (the 3 pulses at 1341.4 MHz being from same radar, apparently). The center frequencies are all within the $\sim$ 50 MHz span between 1315.5 MHz and 1365.8 MHz. It is interesting to note that the radars seem to belong to one of two types: a pulsed CW type generating the $\sim$ 2 μs pulses, and a chirped CW type generating the $\sim$ 60 μs pulses. The pulsed CW type is familiar from similar observations at Columbus, OH and Arecibo, PR [2], where these radars are known to be used for long-range air traffic control. The chirped CW type is familiar from similar observations at Arecibo [1], where a modulation similar in pulse length and bandwidth was observed from an L-88A radar mounted on an Aerostat (balloon) for interdiction of drug smuggling.

Freq MHz	BW MHz	Length μs	Power dBm	Remarks
1315.5	1.0	2	−56	CW
1320.5	1.0	2	−54	CW
1341.4	1.0	2	−56	CW
1341.4	1.0	2	−47	CW, multipath
1341.4	1.0	2	−45	CW, multipath
1341.5	2.0	55	−44	Chirp
1342.5	1.4	60	−54	Chirp
1365.8	1.4	60	−55	Chirp

Fig. 8. Detected pulses from coherent sampling data, sorted by center frequency. "Power" is peak, referenced to the antenna terminals. "Freq," "BW," and "Length" are all approximate.

Note that the detected pulses all exhibit power between −44 dBm and −56 dBm at the antenna terminals. This does not infer that weaker pulses are not present, only that they were not detected. Weaker pulses can be detected by channelizing the 14 MHz passband into subbands of $\sim$ 1 MHz (approximately matched to the observed bandwidth of known radars). This improves

the detection sensitivity by at least 10 dB. When we attempted this, we found three additional pulses from the 1365.8 MHz radar, but no new radars.

VIII. Implications

The results of Section III demonstrate that a simple time "blanking" strategy implemented in a high-dynamic range, high sample rate radiometer may significantly reduce the impact of radio frequency interference on L-band brightness measurements. Further experiments to quantify the level of interference mitigation observed as well as total radiometric performance are planned for 2003. In addition, recent data from the AMSR-E instrument (on the Aqua satellite) C-band channel has shown problems with RFI; applications of similar strategies to radiometers operating at C-band are currently under consideration.

RFI survey results in Sections VI and VII suggest that radar is the dominant problem (although perhaps not the sole problem) below 1400 MHz. Some of these radars were found to be very strong and, despite being well out-of-band, could potentially affect total-power measurements in the $\sim$ 1413 MHz protected band depending on the quality of filtering provided by the radiometer. To observe outside the protected band (for example, to improve sensitivity by increasing bandwidth), it is certainly better from a dynamic range perspective to use the spectrum above the band as opposed to below it. However, we stress that we have not ruled out the possibility that weak yet significant RFI is present on either side of the protected band. Although the spectrum below the protected band is much much worse from a dynamic range perspective, other considerations apply. In particular, we note that pulses associated with any given radar are present only $\sim$ 0.1% of the time. In other words, the spectrum below 1400 MHz is mostly available in a "time-frequency occupancy" sense. Thus, this spectrum can be made available for radiometry with efficiency close to 100% by detecting and blanking radar pulses.

Acknowledgments

The authors are grateful for the assistance of E. Kim of NASA/GSFC and D. Easmunt of Dyncorp (at NASA/WFF) for their assistance in the logistics and conduct of these measurements. This work was supported in part by NASA "Instrument Incubator Program" project NAS5-02001 and in part by the National Science Foundation (NSF) under Award No. AST-0138263. Thanks to J. Cordes, R. Bhat, P. Perillat, and L. Wray for advice and technical support at Arecibo. The Arecibo Observatory is operated by Cornell University under a Cooperative Agreement with the NSF.

References

[1] S.W. Ellingson, *Characterization of Some L-Band Signals Visible at Arecibo*, Technical Report 743467-2,The Ohio State University ElectroScience Laboratory, February 2003.

[2] S.W. Ellingson and G.A. Hampson, "Mitigation of Radar Interference in L-Band Radio Astronomy," *Astrophysical J. Supp.*, in press.

[3] S.W. Ellingson and G.A. Hampson, *RFI and Asynchronous Pulse Blanking in the 1230-1375 MHz Band at Arecibo*, The Ohio State University ElectroScience Laboratory Technical Report 743467-3, Feb 2003.

[4] S. W. Ellingson, G. A. Hampson, and J. T. Johnson, "Design of an Interference Suppressing L-band Microwave Radiometer," *Proc. 2003 IGARSS*, Toulouse.